High-Definition Differential Ion Mobility Spectrometry with Structural Isotopic Shifts for Anionic Compounds

Pratima Pathak, Alexandre A. Shvartsburg*

Department of Chemistry and Biochemistry, Wichita State University, 1845 Fairmount, Wichita, KS 67260

* e-mail: alexandre.shvartsburg@wichita.edu

ABSTRACT: Differential ion mobility spectrometry (FAIMS) had emerged in 2000-s as a novel tool for post-ionization separations in conjunction with mass spectrometry (MS). High-definition FAIMS introduced a decade ago has enabled resolution of peptide, lipid, and other molecular isomers with minute structural variations, and recently the isotopic shift analyses where the spectral pattern for stable isotopes fingerprints the ion geometry. Most studies, including all isotopic shift analyses, were in the positive mode. Here, we achieve the same high resolution for anions exemplified by phthalic acid isomers. The resolving power and magnitude of isotopic shifts are in line with the metrics for analogous haloaniline cations, establishing high-definition negative-mode FAIMS with structurally specific isotopic shifts. Different shifts (including the new ^{18}O) remain additive and mutually orthogonal, demonstrating the generality of those properties across the elements and charge states. Expanding to common (not halogenated) organic compounds is a key step toward the broad use of FAIMS isotopic shift methodology.

The unrivalled combination of universality, specificity, sensitivity, dynamic range, and speed makes MS the leading instrumental platform of analytical chemistry.[1] Still, full characterization and quantification of complex samples routine to modern bio and environmental analyses normally requires prior separations.[2] This particularly holds for the isomer delineation that remains a weak spot of MS relying on ion mass (m). However, the critical role of isomers in biological functionality is increasingly grasped across proteomics, metabolomics, and structural biology.[3,4] Tandem MS methods can distinguish only some isomers that yield informative fragments.[5,6]

Hence, disentangling the isomers tends to fall onto the separation step. That was traditionally implemented via liquid chromatography (LC) or electrophoresis,[2,7] which are versatile yet inherently slow, commonly not selective enough, and hard to replicate because of poorly controlled conditions. Those techniques are increasingly replaced or supplemented by post-ionization ion mobility separations (IMS) that are fast thanks to rapid molecular motion in gases, more reproducible, and offer unique selectivity (the relative separation parameters of species).[8] One can pick the original linear IMS (based on the absolute mobility K at moderate electric field E) or differential or field asymmetric waveform IMS (FAIMS) that captures the difference (ΔK) between K values at two E levels.[8,9]

In FAIMS,[9] a periodic asymmetric waveform with the amplitude (dispersion voltage) U_D is applied across a gap of fixed width g between two electrodes, producing a peak field $E_D = U_D/g$. Ions pushed by gas flow are deflected toward the electrodes and destroyed on impact. For a given species with certain $K(E)$ function, the drift is offset by fixed compensation field (E_C) due to a dc compensation voltage (U_C) superimposed on the waveform. Thus equilibrated ions pass to the MS detector, while others are still eliminated. Scanning $E_C = U_C/g$ elicits the spectrum of species entering the gap. The planar gaps with homogeneous field maximize the resolving power R, which scales as the square root of filtering time t governed by the volume flow rate Q of supplied gas.[9]

The K values at low E can be calculated within ~2%, which lets elucidating the ion structures by comparing the values computed for candidate geometries with linear IMS data.[10] That is not currently feasible with FAIMS as the hugely more complex high-field dynamics of non-thermal ions resists rigorous modeling. However, a tight K/m correlation (reflecting the inherent connection between ion mass and size) limits the linear IMS resolution of isomers and isobars.[11] With a much looser $\Delta K(m)$ dependence,[12] FAIMS at same formal R generally separates similar species better. For example, various lipid classes and peptides with alternative modified sites, sequence inversions, or D/L amino acid substitutions were resolved by FAIMS better than by linear IMS, with m more orthogonal to ΔK than K by ~3 - 6 times.[12,13] A qualitative impact of gas composition on FAIMS selectivity[14] (versus minor deviations in linear IMS)[15] enhances this aspect, creating the flexibility akin to that achieved by modulation of LC mobile phase.

The orthogonality between FAIMS and MS dimensions shines in isotopic separations. While the MS isotopic envelopes convey only the compound formulas, the shifts between isotopologues in FAIMS spectra (ΔE_C) are specific to the ion geometry. We developed this method utilizing the haloanilines that feature isomers with varied halogen positions on the ring and exhibit intense heavy isotopologues comprising abundant ^{37}Cl and/or ^{81}Br atoms.[16-20] Those investigations have revealed the salient isotopic shift properties: (i) feasibility of both signs (set to "+" when absolute E_C decreases for a heavier isotopologue), (ii) profound dependence, including the sign change, on the gas composition, (iii) independence of ΔE_C from the mass increment (e.g., the shifts for ^{13}C substitution at +1 Da may be larger than those for ^{37}Cl or ^{81}Br at +2 Da), (iv) additivity (i.e., ΔE_C for sum of isotopic labels equals the sum of their ΔE_C values), and (v) orthogonality between different elemental shifts (e.g., for

^{13}C and ^{37}Cl) that undergirds superior multidimensional matrices. All tested haloaniline isomers with up to three Cl, Br, or I atoms were distinguished by 2-D shifts, portending well for this novel structural tool.

The isomer-specific peak shifts resulting from the natural stable isotopes (^{37}Cl, ^{81}Br, or ^{13}C) were also observed in linear IMS for the dichloroaniline (DCA), dibromoaniline (DBA), and quaternary ammonium salt cations.[21] However, the relative shifts for same substitutions were smaller in linear IMS than FAIMS: the maxima were 0.66% for $^{37}Cl_2$ in DCAs and 0.30% for $^{81}Br_2$ in DBAs for K but respectively 1.6% and 0.7% for E_C values.[17,19,21] The advantage of FAIMS was greater for diagnostic inter-isomer spreads, which were 0.9% (DCAs) and 0.4% (DBAs) versus 0.13% (DCAs) and 0.04% (DBAs) in linear IMS. Broadly, the heavy isotope substitutions have always diminished mobilities in linear IMS[21-24] (per the reduced mass term in Mason-Schamp equation)[25] but increased or decreased the E_C in FAIMS.[16-20] These findings accord with the generally greater orthogonality of MS to FAIMS than linear IMS.[12,13]

Most organic and biological molecules contain just H, C, N, and/or O atoms. The suitability of FAIMS structural isotopic shift method for such species with less intense heavy isotopologues (resulting from D, ^{13}C, ^{15}N, ^{17}O, and ^{18}O with <1% relative abundance) has been of concern.[20] As with MS in general, most FAIMS/MS studies addressed cations. While FAIMS has separated isomers for anions (e.g., phthalic[26] or haloacetic acids[27] and perfluoroalkyl substances, PFAS[28]), no isotopic shifts were reported - perhaps because of lower E_D, E_C, and R metrics.

Here we extend FAIMS of higher resolving power to the negative mode and explore the isotopic shifts for mainstream (not halogenated) organic compounds.

Experimental Methods

A planar FAIMS cell (g = 1.88 mm) operating at atmospheric pressure and room temperature (~20 °C) is coupled to the Thermo LTQ XL ion trap via a custom electrodynamic ion funnel (IF) interface prefaced by a heated capillary.[6-20] Ions come from an ESI emitter installed in front of the curtain plate/orifice inlet in one of the cell electrodes. To process anions, the MS instrument is placed in the negative mode and the polarity of dc voltages on all IF and cell elements and the emitter is inverted. Then the biases to ground are −140 V (IF entrance), −160 V (MS capillary), −250 V (cell), −1 kV (curtain plate), and −5 kV (emitter). A bisinusoidal waveform (1 MHz frequency, 2:1 harmonics ratio) has U_D = 5.0 kV. Unlike with the curved-gap FAIMS stages,[9,29] the homogeneous field here does not focus/defocus ions and we need not flip the waveform polarity to ensure ion transmission. The U_C windows with ion signal are scanned at the scan rate (Sr) of 1 V/min.

The typical buffers for high-definition FAIMS are[16-20] He/N_2 and He/CO_2. These provide excellent resolution as (i) non-Blanc effects (high-field deviations from the Blanc's law of ion diffusion and mobility, prominent for the mixtures of physically disparate gases) raise absolute E_C values[9] and (ii) the peak widths (scaling as $K^{-1/2}$) decrease in light gases with high K values per the Mason-Schamp equation.[30] Here we use the He/CO_2 mixtures with up to 43% He (v/v) to avoid the arc breakdown, formulated by digital flowmeters with 2 and 5 L/min ranges (MKS Instruments) and purified by a GC filter (Agilent, RMSN-4).

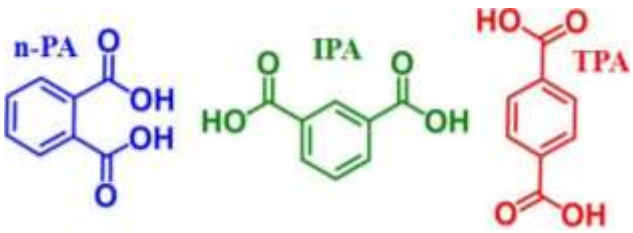

Figure 1. Three phthalic acid isomers probed in this work.

Ions can be reasonably desolvated in the inlet and injected to the FAIMS cell at Q ~ 0.5 - 4 L/min, for t ~ 70 - 600 ms.[31] Per the workflow for parallel cations,[16-20] we adopt Q = 3 L/min (with the ensuing t ~ 100 ms coming at the lower end of operating range) to elevate the ion signal and expand the dynamic range to cover the minor isotopologues. The inevitable slight resolution reduction is less important to these analyses with the isotopologues extracted by MS anyhow.

As with monohaloanilines,[16,18,20] moving two groups on the aromatic ring from ortho to para to meta configuration makes three phthalic acid (PA) isomers (Figure 1): n-PA, iso- (IPA), and tere- (TPA).[27] The standards (Sigma Aldrich) or their mixtures were dissolved to 50 - 100 μM in 1:1 methanol/water with 0.2 mM ammonium acetate and infused to the emitter at 0.5 uL/min. This high concentration maximizes the ion counts to incorporate most isotopic traces. The E_C axis was anchored by linear dilation using the 2-chlorobenzoic acid (156 Da) spiked at 20 μM. The E_C values were taken as the midpoints at peak half-heights, with 10 - 20 replicates acquired for sufficient statistics. Averaging the E_C values obtained at multiple heights and ultimately by numerical integration of the peak can improve the ΔE_C precision,[19,20] but was redundant here.

Results and Discussion

Isotopic envelopes and mass spectra

The negative-mode ESI of acids yields deprotonated ions, seen for PAs with the base peak at m/z = 165 (Figure 2). The *a*

Table 1. Relative intensities computed for $[PA - H]^-$ isotopologues (using the utility on www.sisweb.com).

Heavy Atoms	Exact mass		Unit mass		% at unit m
	m, Da	I*	m, Da	I*	
None	165.0188	**100**	165	100	100
^{13}C	166.0222	**8.65**	166	8.89	97.3
^{17}O	166.0230	**0.160**			1.8
D	166.0251	**0.08**			0.9
^{18}O	167.0231	**0.802**	167	1.15	69.7
$^{13}C_2$	167.0255	**0.328**			28.5
$^{13}C^{17}O$	167.0264	0.014			1.2
^{13}CD	167.0284	0.007			0.6
$^{13}C^{18}O$	168.0264	**0.069**	168	0.079	88
$^{13}C_3$	168.0289	0.007			9
$^{18}O_2$	169.0273	0.0024	169	0.0053	45
$^{13}C_2{}^{18}O$	169.0298	0.0026			49

* Intensity relative to the base peak (100%) for all species with I* ≥ 0.002%. The I* values ≥0.02% are bolded.

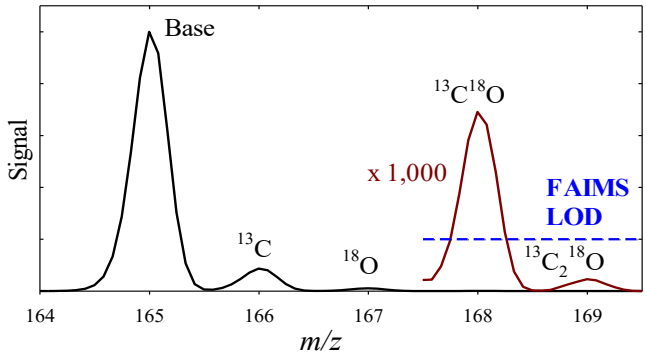

Figure 2. Normalized mass spectrum for TPA with the trace at $m/z > 167.5$ scaled up as marked. The signal threshold of 0.02% for useful FAIMS data is shown.

priori isotopic distribution for $[PA - H]^-$ ions (Table 1) features a peak at $m/z = 166$ with 9% relative intensity, nearly all due to the ^{13}C isotope. The next peak at $m/z = 167$ with 1.2% intensity is split between the compositions with ^{18}O and $^{13}C_2$ in 70/29 ratio - by far the smallest for nominally isobaric species in our isotopic shift analyses to date. The peak at $m/z = 168$ with 0.08% intensity is dominated by the $^{13}C^{18}O$ isotopologues combining the above ^{13}C and ^{18}O substitutions. With all isobaric isotopologues merged, the measured mass spectra match the projections for intensities at unit masses (Figure 2).

The minimal isotopic abundance for FAIMS/MS analyses exceeds the MS limit of detection because of losses in the FAIMS cell and spread of signal into numerous E_C bins (including the empty ones). The minimum for this system has been[17] ~0.02%. Likewise here, we got useful FAIMS spectra for the peak at $m/z = 168$ but not that at 169 with 0.005% intensity. Therefore, the Table 1 concludes at that mass.

FAIMS separations

The peaks for all isomers lie above the raw bias voltage, i.e., at smaller absolute negative voltages. This means the mobility increasing at higher E (called type A ions), which is standard for species up to ~300 Da in He/CO_2 buffers.[9,16-20] This situation was defined as negative U_C and E_C for cations, a convention retained here. All isomers move to more negative E_C values upon He addition, eventually reaching $|E_C| > 200$ V/cm and R ~80 (Figure 3). These behaviors and parameters track those for similar 1+ cations such as haloanilines.[16-20] Present resolving power is well beyond that in preceding FAIMS analyses of anions ($R < 30$ for PFAS[28] and much less in earlier work[26,27]).

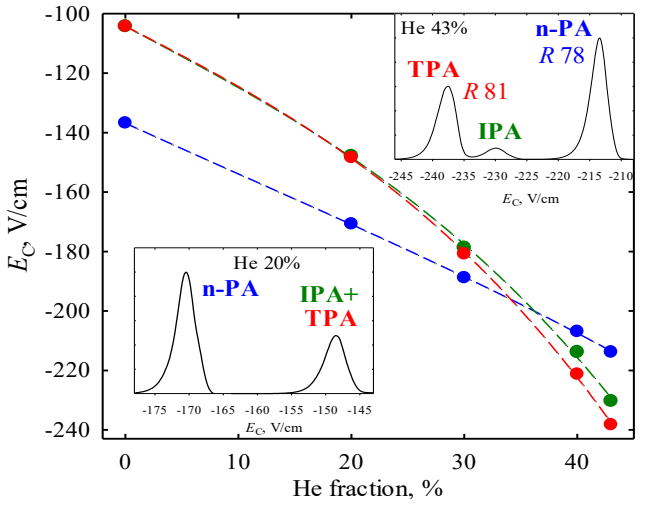

Figure 3. Measured E_C values for PAs (at $m/z = 165$), lines are cubic regressions. The spectra at 20% and 43% He are plotted, with R values marked for the latter.

These curves steepen from n-PA to IPA to TPA, the last two lying close. The $|E_C|$ values are much greater for n-PA than IPA and TPA in CO_2 and vice versa at 43% He, with all isomers merging at ~35% He. Such peak order inversion was not encountered for haloanilines in He/CO_2 buffers,[16-20] but was noted for PAs in N_2/CO_2 buffers[27] and might be a facet of PAs. With the IPA and TPA merging under ~30% He, the overall resolution maximizes at the highest He fraction as usual (exceeding baseline at 43% He). At <30% He, one can separate n-PA from the (IPA + TPA) mixture (Figure 3).

Isotopic shifts

The ^{13}C shifts for all isomers extracted at $m/z = 166$ are positive (i.e., the $|E_C|$ values drop as the peaks transpose to more negative raw CVs) and rise upon He addition (Figure 4a). This

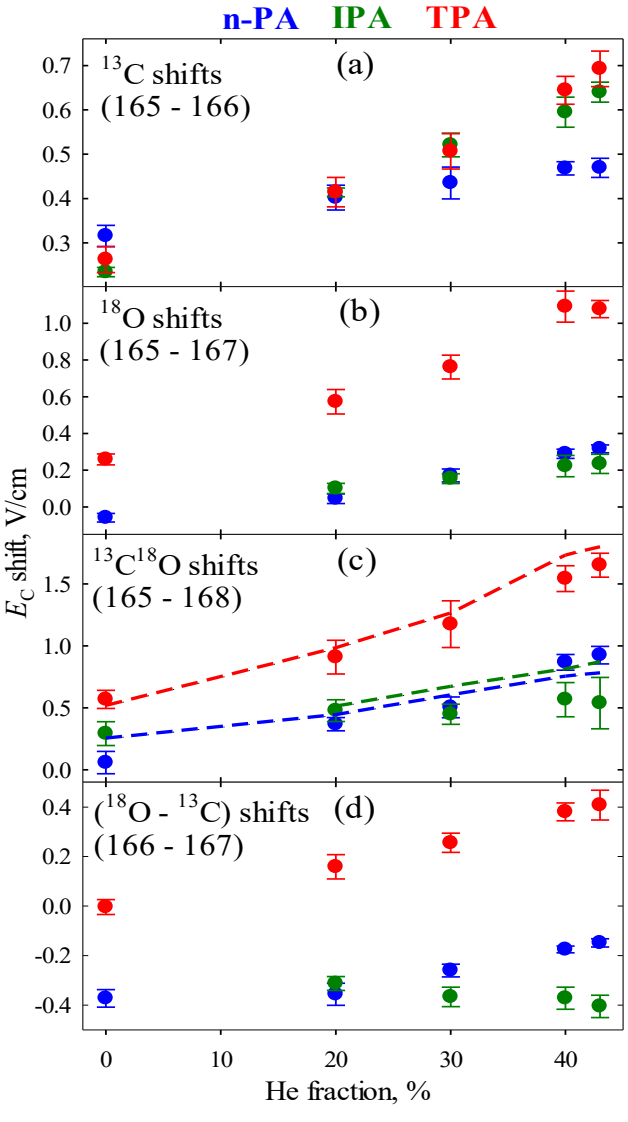

Figure 4. Measured ΔE_C in PAs for the 165 - 166 (a), 165 - 167 (b), 165 - 168 (c), and 166 - 167 (d) shifts with major isotopic substitutions labeled. Dashed lines in (c) show the sum of shifts from (a) and (b). Error bars mark the 95% confidence intervals.

resembles the pattern for monochloroanilines,[16,18] but here the shifts are smaller (as anticipated for heavier ions) and vary over isomers less. The ΔE_C differences are insufficient to pull IPA and TPA apart, but readily distinguish both from n-PA with smaller shifts at 40 - 43% He. The trends across gas composition intriguingly mirror those for absolute E_C values (Figure 3): both $|E_C|$ and ΔE_C rank as IPA ≅ TPA < n-PA in CO_2 and n-PA < IPA < TPA at 43% He.

No ^{17}O or ^{18}O shifts were previously encountered in FAIMS spectra. The isotopologue with ^{17}O constituting <2% of the peak at m/z = 166 (Table 1) can't materially affect its measured E_C, especially that determined at half-maximum. Indeed, those peaks in FAIMS spectra are not split or visibly tailing. The species with ^{18}O makes 70% of peak at m/z = 167 and should substantially set the E_C at half-maximum. The associated shifts are also positive (save for n-PA and IPA in CO_2 with marginally negative ΔE_C) and increase upon He addition (Figure 4b). The mean 95% confidence interval for ^{18}O shifts is 0.042 V/cm (or 19%) vs. 0.027 V/cm (or 6%) for the ^{13}C shifts, reflecting a 10× lower abundance of the ^{18}O isotopologues. Nonetheless, the ^{18}O shifts fit clear trend lines: those for n-PA and IPA are near-identical and consistently well below that for TPA. Hence, together the ^{13}C and ^{18}O shifts distinguish all three isomers. A significant $^{13}C_2$ contamination likely influences the shifts at m/z = 167, but with additivity $\Delta E_C(^{13}C_2)$ ought to equal $2\Delta E_C(^{13}C)$. Then the dissimilar shifts at m/z of 166 and 167 support the latter being primarily defined by the ^{18}O isotopologues.

The pattern of $^{13}C^{18}O$ shifts at m/z = 168 (Figure 4c) resembles that for ^{18}O: close low positive shifts for n-PA and IPA but much higher ΔE_C for TPA clearly delineated despite the wide confidence interval (mean of 0.10 V/cm or 26%) due to low signal (0.08% of the base peak). The measured values expectedly track the $[\Delta E_C(^{13}C) + \Delta E_C(^{18}O)]$ lines within the combined uncertainty of all three shifts.

The best isomer delineation may be delivered by hybrid shifts aggregating multiple isotopic substitutions. Here, the (^{18}O – ^{13}C) shifts between m/z of 166 and 167 firmly distinguish all isomers at 40 - 43% He (Figure 4d).

The evolution of several isotopic shifts across gas compositions is succinctly depicted in 2-D maps.[17,19] The isolated domains in $^{13}C/^{18}O$ shift map instantly demarcate all PA isomers with any He/CO_2 buffer tried (Figure 5).

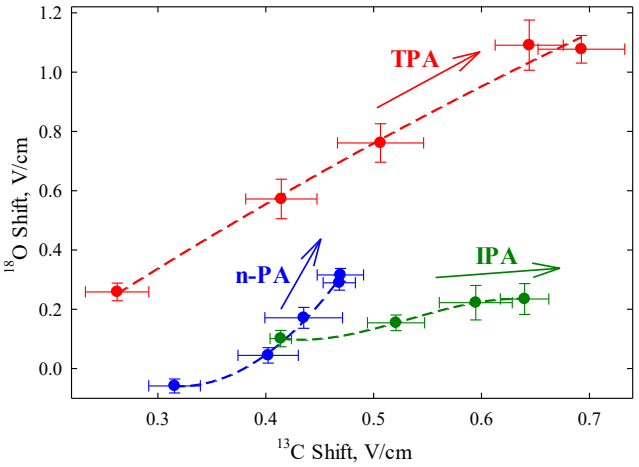

Figure 5. The $^{13}C/^{18}O$ shift map for PAs across gas compositions. Error bars mark the 95% confidence intervals. Arrows point in the direction of increasing He fraction.

Conclusions

We have achieved FAIMS of anions with same high resolution as for cations, illustrated for the phthalic acid (PA) isomers. This would advance the analyses of species in the negative mode, such as of organic acids including the humic/fulvic acids central to the natural organic matter,[32] halogenated moieties (topical to environmental monitoring and toxicology),[27,28] organophosphates, nitro compounds including explosives targeted in security screenings,[33] many lipids (e.g., phosphatidylinositols and sulfatides),[34] and oligonucleotides.[35] Such FAIMS separations can be coupled to photoelectron or threshold photodetachment spectroscopy for complementary structural insights, as realized with linear IMS.[36,37]

The FAIMS spectra for PA anions exhibit structurally specific ^{13}C and ^{18}O shifts permitting complete isomer delineation. The orthogonality and additivity properties follow those for elemental shifts in cations.[16-20] The shifts for PAs compare in magnitude with those for similarly sized cations in He/CO_2 buffers and also increase at higher He fractions. These observations, including the first for ^{18}O shifts, show the breadth of isotopic shifts and their principal characteristics. The expansion to regular (non-halogenated) organics opens the door to broad deployment of the structural isotopic shift approach.

The isotopic shifts in both linear IMS and FAIMS seem related to the ion center of mass moving within the geometry frame.[16,21,24] However, the order of shifts for same DCA isomers differed,[17,21] evidencing the orthogonality between the shifts in two separations. Hence, using the 2-D FAIMS/IMS platforms[38] to measure the most specific $\Delta K/\Delta E_C$ shifts appears promising.

ACKNOWLEDGMENT

This research was funded by NSF (CHE-2105182). We thank Gordon A. Anderson (GAACE) and Hayden Thurman (WSU) for experimental help.

REFERENCES

1. Gross, J. H. *Mass Spectrometry - a Textbook*; Springer, **2017**.
2. Pitt, J. J. Principles and Applications of Liquid Chromatography - Mass Spectrometry in Clinical Biochemistry. *Clin. Biochem. Rev.* **2009**, *30*, 19.
3. Jenuwein, T.; Allis, C. D. Translating the Histone Code. *Science* **2001**, *293*, 1074.
4. Chatgilialoglu, C.; Ferreri, C.; Melchiorre, M.; Sansone, A.; Torreggiani, A. Lipid Geometrical Isomerism: from Chemistry to Biology and Diagnostics. *Chem. Rev.* **2014**, *114*, 255.
5. Xuan, Y.; Creese, A. J.; Horner, J. A.; Cooper, H. J. High-Field Asymmetric Waveform Ion Mobility Spectrometry (FAIMS) Coupled with High-Resolution Electron Transfer Dissociation Mass Spectrometry for the Analysis of Isobaric Phosphopeptides. *Rapid. Commun. Mass Spectrom.* **2009**, *23*, 1963.
6. Bowman, A. P.; Abzalimov, R. R.; Shvartsburg, A. A. Broad Separation of Isomeric Lipids by High-Resolution Differential Ion Mobility Spectrometry with Tandem Mass Spectrometry. *J. Am. Soc. Mass Spectrom.* **2017**, *28*, 1552.
7. Bird, S. S.; Marur, V. R.; Stavrovskaya, I. G.; Kristal, B. S. Separation of Cis-Trans Phospholipid Isomers Using Reversed Phase LC with High Resolution MS Detection. *Anal. Chem.* **2012**, *84*, 5509.
8. Eiceman, G. A., Karpas, Z., Hill, H. H. *Ion Mobility Spectrometry*; CRC Press: Boca Raton, FL, **2013**.
9. Shvartsburg, A. A. *Differential Ion Mobility Spectrometry*; CRC Press: Boca Raton, FL, **2008**.

10. Ruotolo, B. T.; Benesch, J. L. P.; Sandercock, A. M.; Hyung, S. J.; Robinson, C. V. Ion Mobility - Mass Spectrometry Analysis of Large Protein Complexes. *Nat. Protocols* **2008**, *3*, 1139.

11. Harris, R. A.; Leaptrot, K. L.; May, J. C.; McLean, J. A. New Frontiers in Lipidomics Analyses Using Structurally Selective Ion Mobility - Mass Spectrometry. *Trends Analyt. Chem.* **2019**, *116*, 316.

12. Shvartsburg, A. A.; Isaac, G.; Leveque, N.; Smith, R. D.; Metz, T. O. Separation and Classification of Lipids Using Differential Ion Mobility Spectrometry. *J. Am. Soc. Mass Spectrom*. **2011**, *22*, 1146.

13. Berthias, F.; Baird, M. A.; Shvartsburg, A. A. Differential Ion Mobility Separations of D/L Peptide Epimers. *Anal. Chem*. **2021**, *93*, 4015.

14. Barnett, D. A.; Ells, B.; Guevremont, R.; Purves, R. W.; Viehland, L. A. Evaluation of Carrier Gases for Use in High-Field Asymmetric Waveform Ion Mobility Spectrometry. *J. Am. Soc. Mass Spectrom.* **2000**, *11*, 1125.

15. Ruotolo, B. T.; McLean, J. A.; Gillig, K. J.; Russell, D. H. Peak Capacity of Ion Mobility Mass Spectrometry: the Utility of Varying Drift Gas Polarizability for the Seperation of Tryptic Peptides. *J. Mass Spectrom.* **2004**, *39*, 361.

16. Kaszycki, J. L.; Baird, M. A.; Shvartsburg, A. A. Molecular Structure Characterization by Isotopic Splitting in Nonlinear Ion Mobility Spectra. *Anal. Chem.* **2018**, *90*, 669.

17. Pathak, P.; Baird, M. A.; Shvartsburg, A. A. Identification of Isomers by Multidimensional Isotopic Shifts in High-Field Ion Mobility Spectra. *Anal. Chem.* **2018**, *90*, 9410.

18. Baird, M. A.; Pathak, P.; Shvartsburg, A. A. Elemental Dependence of Structurally Specific Isotopic Shifts in High-Field Ion Mobility Spectra. *Anal. Chem*. **2019**, *91*, 3687.

19. Pathak, P.; Baird, M. A.; Shvartsburg, A. A. Structurally Informative Isotopic Shifts in Ion Mobility Spectra for Heavier Species. *J. Am. Soc. Mass Spectrom.* **2020**, *31*, 137.

20. Pathak, P.; Sarycheva, A.; Baird, M. A.; Shvartsburg, A. A. Delineation of Isomers by the ^{13}C Shifts in Ion Mobility Spectra. *J. Am. Soc. Mass Spectrom*. **2021**, *32*, 340.

21. Williamson, D. L., Nagy, G. Isomer and Conformer-Specific Mass Distribution-Based Isotopic Shifts in High-Resolution Cyclic Ion Mobility Separations. *Anal. Chem.* **2022**, *94*, 12890.

22. Kirk, A. T.; Raddatz, C. R.; Zimmermann, S. Separations of Isotopologues in Ultra-High-Resolution Ion Mobility Spectrometry. *Anal. Chem.* **2017**, *89*, 1509.

23. Wojcik, R.; Nagy, G.; Attah, I. K.; Webb, I. K.; Garimella, S. V. B.; Weitz, K. K.; Hollerbach, A.; Monroe, M. E.; Ligare, M. R.; Nielson, F. F., et al. SLIM Ultrahigh Resolution Ion Mobility Spectrometry Separations of Isotopologues and Isotopomers Reveal Mobility Shifts due to Mass Distribution Changes. *Anal. Chem.* **2019**, *91*, 11952.

24. Harrilal, C. P.; Gandhi, V. D.; Nagy, G.; Chen, X.; Buchanan, M. G.; Wojcik, R.; Conant, C. R.; Donor, M. T.; Ibrahim, Y. M.; Garimella, S. V. B., et al. Measurement and Theory of Gas-Phase Ion Mobility Shifts Resulting from Isotopomer Mass Distribution Changes. *Anal. Chem.* **2021**, *93*, 14966.

25. Valentine, S. J.; Clemmer, D. E. Treatise on the Measurement of Molecular Masses with Ion Mobility Spectrometry. *Anal. Chem.* **2009**, *81*, 5876.

26. Barnett, D. A.; Purves, R. W.; Ells, B.; Guevremont, R. Separation of o-, m-, and p- Phthalic Acids by High-Field Asymmetric Waveform Ion Mobility Spectrometry (FAIMS) Using Mixed Carrier Gases. *J. Mass Spectrom.* **2000**, *35*, 976.

27. Gabryelski, W.; Wu, F.; Froese, K. L. Comparison of High-Field Asymmetric Waveform Ion Mobility Spectrometry with GC Methods in Analysis of Haloacetic Acids in Drinking Water. *Anal. Chem.* **2003**, *75*, 2478.

28. Ahmed, E.; Kabir, K. M. M.; Wang, H.; Xiao, D.; Fletcher, J.; Donald, W. A. Rapid Separation of Isomeric Perfluoroalkyl Substances by High-Resolution Differential Ion Mobility Spectrometry. *Anal. Chim. Acta* **2019**, *1058*, 127.

29. Guevremont, R.; Purves, R. W. Atmospheric Pressure Ion Focusing in a High-Field Asymmetric Waveform Ion Mobility Spectrometer. *Rev. Sci. Instrum.* **1999**, *70*, 1370.

30. Shvartsburg, A. A.; Smith, R. D. Scaling of the Resolving Power and Sensitivity for Planar FAIMS and Mobility-Based Discrimination in Flow- and Field- Driven Analyzers. *J. Am. Soc. Mass Spectrom.* **2007**, *18*, 1672.

31. Shvartsburg, A. A.; Tang, K.; Smith, R. D. FAIMS Operation for Realistic Gas Flow Profile and Asymmetric Waveforms Including Electronic Noise and Ripple. *J. Am. Soc. Mass Spectrom.* **2005**, *16*, 1447.

32. Stenson, A. C.; Landing, W. M.; Marshall, A. G.; Cooper, W. T. Ionization and Fragmentation of Humic Substances in Electrospray Ionization Fourier Transform-Ion Cyclotron Resonance Mass Spectrometry. *Anal. Chem.* **2002**, *74*, 4397.

33. Forbes, T. P.; Sisco, E. Recent Advances in Mass Spectrometry of Trace Explosives. *Analyst* **2018**, *143*, 1948.

34. Angel, P. M.; Spraggins, J. M.; Baldwin, H. S.; Caprioli, R. Enhanced Sensitivity for High Spatial Resolution Lipid Analyses by Negative Ion Mode Matrix Assisted Laser Desorption Ionization Imaging Mass Spectrometry. *Anal. Chem*. **2012**, *84*, 1557.

35. McLuckey, S. A.; Van Berkel, G. J.; Glish, G. L. Tandem Mass Spectrometry of Small, Multiply Charged Oligonucleotides. *J. Am. Soc. Mass Spectrom.* **1992**, *3*, 60.

36. Fromherz, R.; Ganteför, G.; Shvartsburg, A. A. Isomer-Resolved Ion Spectroscopy. *Phys. Rev. Lett.* **2002**, *89*, 083001.

37. Vonderach, M.; Ehrler, O. T.; Weis, P.; Kappes, M. M. Combining Ion Mobility Spectrometry, Mass Spectrometry, and Photoelectron Spectroscopy in a High-Transmission Instrument. *Anal. Chem.* **2011**, *83*, 1108.

38. Tang, K.; Li, F.; Shvartsburg, A. A.; Strittmatter, E. F.; Smith, R. D. Two-Dimensional Gas-Phase Separations Coupled to Mass Spectrometry for Analysis of Complex Mixtures. *Anal. Chem*. **2005**, *77*, 6381.

TOC Graphics